Sidewall inclined slot in a rectangular waveguide: Theory and experiment

Article *in* IEE Proceedings - Microwaves Antennas and Propagation · July 1998

DOI: 10.1049/ip-map:19981956 · Source: IEEE Xplore

CITATIONS
12

READS
114

3 authors:

Vaidya Shikha Prakash
Padaav Speciality Ayurvedic Treatment Center
51 PUBLICATIONS **2,458** CITATIONS
SEE PROFILE

Somita Christopher
CARE Hospitals
26 PUBLICATIONS **68** CITATIONS
SEE PROFILE

Narayanaswamy Balakrishnan
Indian Institute of Science
209 PUBLICATIONS **2,351** CITATIONS
SEE PROFILE

Sidewall inclined slot in a rectangular waveguide: Theory and experiment

V.V.S. Prakash
S. Christopher
N. Balakrishnan

Indexing terms: Rectangular waveguides, Admittance, Edge slots, Finite difference method, Method of moments

Abstract: A novel analysis to compute the admittance characteristics of the slots cut in the narrow wall of a rectangular waveguide, which includes the corner diffraction effects and the finite waveguide wall thickness, is presented. A coupled magnetic field integral equation is formulated at the slot aperture which is solved by the Galerkin approach of the method of moments using entire domain sinusoidal basis functions. The externally scattered fields are computed using the finite difference method (FDM) coupled with the measured equation of invariance (MEI). The guide wall thickness forms a closed cavity and the fields inside it are evaluated using the standard FDM. The fields scattered inside the waveguide are formulated in the spectral domain for faster convergence compared to the traditional spatial domain expansions. The computed results have been compared with the experimental results and also with the measured data published in previous literature. Good agreement between the theoretical and experimental results is obtained to demonstrate the validity of the present analysis.

1 Introduction

One of the most widely used waveguide radiating elements for array antennas is the sidewall inclined slot (narrow wall slot) in a rectangular waveguide. A number of investigations are reported on the impedance properties of these slots [1–7]. For slot lengths corresponding to first resonance, a portion of the slot extends onto the top and the bottom broad faces of the waveguide and this complicates the analysis. Stevenson [1] assumed that the slot resonates at half the free-space wavelength ($\lambda_0/2$) and arrived at a simple expression for the resonant conductance by neglecting the parts of the slot cut on the broad walls. Das *et al.* [2] derived an expression for the slot admittance using a plane wave spectrum expansion of the slot in an infinite ground plane. They neglected the internal self reaction and concluded that the slot resonant length is constant irrespective of the slot tilt. Hsu and Chen [3] added the missing internal self reaction term but made the same approximation that the slot is cut on an infinite ground plane. The internal self reaction was represented by a diverging series leading to inaccurate results. Jan *et al.* [4, 5] used 90° wedge Green's functions to account for the waveguide corners. They neglected the mutual interaction between the waveguide corners, which is considerable due to the close proximity of the corners on the narrow wall, and the finite wall thickness of the waveguide was not considered. Recently, a more complicated variational reaction formulation for edge slots was developed by using subsectional basis functions where account is taken of the wall thickness using the finite element method [6]. The external fields are evaluated using 90° wedge Green's functions only, while the internal fields are computed using Stevenson's Green's functions in the spatial domain. There is around 5–10% error in the computation of the slot admittance between the theory and experiment. Also there is a shift of 50MHz between the theory and experiment in the resonant frequency. Ahn [7] used the method of moments approach for the analysis of a narrow wall slot on a rectangular waveguide. Wang and Sangster [8] used the finite element technique to model a slot scatterer in a thick-walled waveguide. In 1997, the effect of the waveguide outer cross-section on the broadwall radiating slot was studied by Prakash *et al.* using the spectrum of two-dimensional solutions for modelling the external scattered fields [9].

In this paper, the slot aperture field is expanded into entire domain sinusoidal functions. The enforcement of the continuity of tangential field components leads to a coupled integral equation formulation with the slot aperture electric field as the unknown, which is solved using the Galerkin method. The effects of the wall thickness, waveguide corners and the folding over of the slot on the top and bottom broadwalls are properly accounted for using a combination of the spectrum of two-dimensional solutions (S2DS), finite differences (FD) and measured equation of invariance (MEI) methods [9–13]. This procedure rigorously evaluates the interaction between all the four exterior corners of the waveguide. The cavity fields are evaluated by solving Helmholtz's equation for the vector potential using FDM. A novel spectral domain Green's function has been derived for the evaluation of internally scattered fields leading to a rapidly converging series form for

IEE Proceedings online no. 19981956

Paper first received 30th June and in revised form 23rd December 1997

V.V.S. Prakash and S. Christopher are with Radar-C, LRDE, C.V. Raman Nagar, Bangalore 560 093, India

N. Balakrishnan is with the Super Computer Education Research Center, Indian Institute of Science, Bangalore, India

the internally scattered fields. The admittance properties of the narrow wall slot are computed from the aperture electric field distribution. Extensive experimental studies are carried out on the isolated edge slot in the S-band. The computed slot conductance and the susceptance are compared with available theoretical and experimental data. Good agreement between the theoretical results and the experimental data has been observed which validates the present analysis.

2 Formulation

The geometry of the edge slot cut on a rectangular waveguide is shown in Fig. 1. The depth of penetration of the slot on the broad wall is δ and it is assumed that only the E_ξ component of the electric field exists in the slot and is constant along the width. The total slot length is $2L$ out of which $2L_1$ is on the narrow wall. The slot is excited by a TE_{10} mode from one end while the other end is matched terminated. The interior surface and the exterior surfaces of the slot are denoted by S_i and S_e, respectively, and the cavity region of the slot formed due to the finite waveguide wall thickness is denoted by V_c.

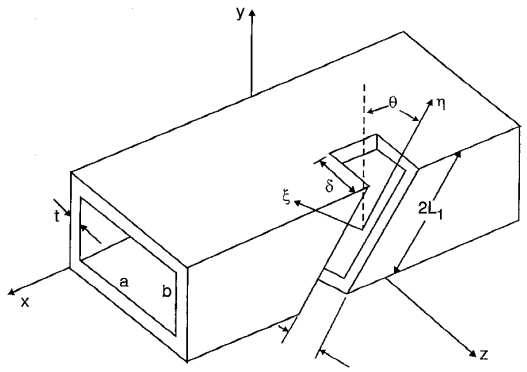

Fig. 1 *Geometry of sidewall inclined slot in a rectangular waveguide*

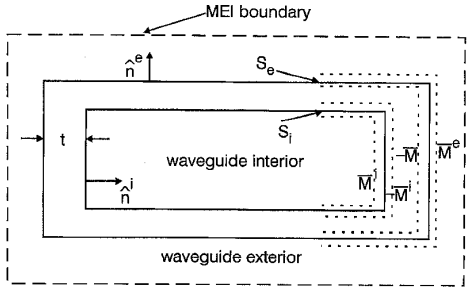

Fig. 2 *Cross-sectional view of the waveguide showing equivalent magnetic currents at the location of the slot*

Using the equivalence principle, the slot is closed by a perfect electric conductor. To ensure the continuity of the tangential electric fields at the slot location, a set of magnetic current sheets are placed at the slot apertures as shown in Fig. 2. This procedure decouples the original domain of the problem into three separate regions, namely

(*a*) the region interior to the waveguide

(*b*) the region exterior to the waveguide

(*c*) the cavity region formed due to the waveguide wall thickness.

The surface magnetic currents are expanded in terms of the entire domain sinusoidal basis functions as follows:

$$\bar{\mathbf{M}}^i = \sum_{q=1}^{N} \alpha_q \bar{\mathbf{f}}_q^i$$

$$\bar{\mathbf{M}}^e = \sum_{q=1}^{N} \beta_q \bar{\mathbf{f}}_q^e \tag{1}$$

where α_q and β_q are the unknown complex expansion coefficients and $\bar{\mathbf{f}}_q^{i,e}$ are the entire domain sinusoidal basis functions corresponding to the interior (S_i) and the exterior (S_e) surfaces given by

$$\bar{\mathbf{f}}_q^u = \sin\left[\frac{q\pi}{2L_u}(s_u + L_u)\right]\hat{\mathbf{s}}^u \tag{2}$$

for $-L_u \leq s_u \leq +L_u$, where s_u is the co-ordinate along the slot length in which the origin is located at the centre of the slot, $\hat{\mathbf{s}}^u$ is the unit tangential vector along the increasing s_u and $u = i$ or e for the internal and the external apertures, respectively.

A set of coupled integral equations is obtained by matching the tangential magnetic fields at the slot apertures S_i and S_e.

$$[\bar{\mathbf{H}}_{int}^{scat}(\bar{\mathbf{M}}^i) + \bar{\mathbf{H}}_{10}^{inc}]\hat{\mathbf{s}}^i = [\bar{\mathbf{H}}^c(-\bar{\mathbf{M}}^i) + \bar{\mathbf{H}}^c(-\bar{\mathbf{M}}^e)]\hat{\mathbf{s}}^i \tag{3}$$

$$\bar{\mathbf{H}}_{ext}^{scat}(\bar{\mathbf{M}}^e)\hat{\mathbf{s}}^e = [\bar{\mathbf{H}}^c(-\bar{\mathbf{M}}^i) + \bar{\mathbf{H}}^c(-\bar{\mathbf{M}}^e)]\hat{\mathbf{s}}^e \tag{4}$$

where $\bar{\mathbf{H}}_{int,ext}^{scat}$ are the internally and externally scattered magnetic fields, $\bar{\mathbf{H}}^c$ is the cavity magnetic field generated by the respective magnetic currents and $\bar{\mathbf{H}}_{10}^{inc}$ is the magnetic field of the incident TE_{10} mode.

The coupled integral equations of eqns. 3 and 4 are solved using Galerkin's approach of the method of moments by an appropriate choice of weighting functions $\bar{\mathbf{f}}_p^{i,e}$, $p = 1, 2, \ldots, N$. A set of linear algebraic equations is obtained by taking the inner product of eqns. 3 and 4 with respect to the weighting functions. These equations are written in matrix form as

$$\begin{bmatrix} [\mathbf{Y}^{int} + \mathbf{Y}^{ii}] & [\mathbf{Y}^{ie}] \\ [\mathbf{Y}^{ei}] & [\mathbf{Y}^{ext} + \mathbf{Y}^{ee}] \end{bmatrix} \begin{bmatrix} [\alpha] \\ [\beta] \end{bmatrix} = \begin{bmatrix} [-\mathbf{h}^{inc}] \\ [0] \end{bmatrix} \tag{5}$$

where each of the elements indicated by $\mathbf{Y}$ is a submatrix of $N \times N$ size. The individual elements of the admittance matrices are expressed in terms of the inner product over the respective slot surface (S_i or S_e). The system of equations given in eqn. 5 is solved for the expansion coefficients α and β of the surface magnetic currents. The slot discontinuity is modelled as an equivalent normalised shunt admittance which is computed from the slot reflection coefficient B/A corresponding to the TE_{10} mode as

$$\bar{y} = \bar{g} + j\bar{b} = \frac{-2B/A}{1 + B/A} \tag{6}$$

2.1 Computation of Y^{int} matrix elements

The internal admittance matrix involves the computation of the scattered magnetic field interior to the waveguide due to the surface magnetic current $\bar{M}^i$ placed at the location of the slot. Traditionally the waveguide interior problems are solved using Stevenson's Green's functions which are formulated in the spatial domain [1]. These Green's functions are in the form of infinite double summations over all the

waveguide modes and present a very slowly converging series or a diverging series due to source singularity. A novel approach using spectral domain waveguide Green's functions is presented here for computing the internal admittance matrix which is found to be rapidly converging and is computationally efficient [14]. Let us define the Fourier transform pair as

$$\tilde{\bar{\mathbf{F}}}(k_z) = \int_z \bar{\mathbf{F}}(z) e^{jk_z z} dz \tag{7}$$

$$\bar{\mathbf{F}}(z) = \frac{1}{2\pi} \int_{k_z} \tilde{\bar{\mathbf{F}}}(k_z) e^{-jk_z z} dk_z \tag{8}$$

The electric field is expressed in terms of the electric vector potential as $\bar{\mathbf{E}} = -\nabla \times \bar{\mathbf{F}}$. Helmholtz's equation for the electric vector potential in the spectral domain is given by

$$\nabla_t^2 \tilde{\bar{\mathbf{F}}}_q + (k_o^2 - k_z^2) \tilde{\bar{\mathbf{F}}}_q = -\tilde{\bar{\mathbf{f}}}_q^i \tag{9}$$

where $\tilde{\mathbf{f}}_q^i$ is the Fourier transformed qth expansion function of the magnetic current $\overline{\mathbf{M}}^i$, $\tilde{\bar{\mathbf{F}}}_q$ is the potential due to it and k_0 is the free space wave number subjected to the boundary condition $\hat{\mathbf{n}}^i \times (\nabla_t - jk_z \hat{\mathbf{z}}) \times \tilde{\bar{\mathbf{f}}}_q^i = 0$ on the surface of the waveguide. The final expression for $\tilde{\bar{\mathbf{F}}}_q$ is given by [14],

$$\tilde{\bar{\mathbf{F}}}_q(\rho, k_z) = \int_s \tilde{\bar{\bar{\mathbf{g}}}}(\rho, \rho', k_z) \tilde{\bar{\mathbf{f}}}_q^i(\rho', k_z) ds \tag{10}$$

where

$$\begin{aligned} \tilde{\bar{\bar{\mathbf{g}}}} = \sum_m \sum_n & \frac{\varepsilon_m \varepsilon_n}{ab(k_z^2 + \Gamma_{mn}^2)} \\ & \times [S_x C_y S_{x'} C_{y'} \hat{\mathbf{x}}\hat{\mathbf{x}} \\ & + C_x S_y C_{x'} S_{y'} \hat{\mathbf{y}}\hat{\mathbf{y}} \\ & + C_x C_y C_{x'} C_{y'} \hat{\mathbf{z}}\hat{\mathbf{z}}] \end{aligned} \tag{11}$$

and

$$\begin{aligned} k_x &= \frac{m\pi}{a}, \quad k_y = \frac{n\pi}{b} \\ S_x &= \sin(k_x x); \quad S_y = \sin(k_y y) \\ C_x &= \cos(k_x x); \quad C_y = \cos(k_y y) \\ \Gamma_{mn}^2 &= k_x^2 + k_y^2 - k_o^2 \end{aligned}$$

The internally scattered magnetic field is expressed in terms of $\tilde{\bar{\mathbf{F}}}_q$ as

$$\begin{aligned} \bar{\mathbf{H}}_{int}^{scat} &= \frac{1}{jk_o \eta_o 2\pi} \int_{k_z=-\infty}^{\infty} [k_o^2 + (\nabla_t - jk_z \hat{\mathbf{z}}) \\ &\qquad \times (\nabla_t - jk_z \hat{\mathbf{z}})] \tilde{\bar{\mathbf{F}}}_q \exp[-jk_z z] dk_z \\ &= \frac{1}{2\pi} \int_{k_z=-\infty}^{\infty} \tilde{\bar{\mathbf{H}}}_{int}^{scat} \exp[-jk_z z] dk_z \end{aligned} \tag{12}$$

The resulting internal admittance matrix elements are obtained by taking the inner product of eqn. 12 with respect to the weighting function $\bar{\mathbf{f}}_p^i$. The (p, q)th element of matrix $[Y^{int}]$ is

$$\begin{aligned} Y_{pq}^{int} &= \int_{S_a} \bar{\mathbf{H}}_{int}^{scat}(\bar{\mathbf{f}}_q^i) \bar{\mathbf{f}}_p^i da \\ &= \frac{1}{2\pi} \int_{k_z} \int_{s_i} \tilde{\bar{\mathbf{f}}}_p^i(-k_z) \tilde{\bar{\mathbf{H}}}_{int}^{scat}(\bar{\mathbf{f}}_q^i) ds dk_z \\ &= \frac{1}{2\pi} \int_{k_z} \tilde{Y}_{pq}^{int}(k_z) dk_z \end{aligned} \tag{13}$$

where 'da' denotes the differential area of the surface S_i and 'ds' denotes the differential length directed along the unit vector $\hat{\mathbf{s}}^i$.

2.2 Computation of Y^{ext} matrix elements

The external admittance matrix involves the computation of the scattered magnetic field exterior to the waveguide due to the surface magnetic current $\overline{\mathbf{M}}^e$ placed at the location of the slot. The externally scattered fields are computed using spectrum of two-dimensional solution method [9–12]. Here, the fields and the sources are Fourier-transformed along the longitudinal axis of the waveguide thereby converting the original three-dimensional problem into a two-dimensional problem with harmonic z-variation. The resulting two-dimensional problem is solved using FDM with the measured equation of invariance as the equation governing the absorbing boundary [13]. This procedure rigorously evaluates the interaction between all the four exterior corners of the waveguide and deviates from the approach of solving for the unknown surface electric currents using the equivalence principle as found in the literature [10–12].

The fields exterior to an infinitely long waveguide of rectangular cross-section can be represented in terms of the electric vector potential F_z and the magnetic vector potential A_z. This corresponds to dividing the original field into TE and TM waves. Following the Fourier transformation with respect to the z-axis, the fields in the spectral domain are governed by the two-dimensional scalar wave equation

$$[\nabla_t^2 + k_\rho^2] \begin{bmatrix} \tilde{F}_z^q \\ \tilde{A}_z^q \end{bmatrix} = 0 \tag{14}$$

where superscript 'q' indicates that the magnetic current $\tilde{\bar{\mathbf{f}}}_q^e = \tilde{\bar{\mathbf{E}}}_{ext}^q \times \hat{\mathbf{n}}^e$ is the source of the potentials $\tilde{F}_z^q$ and $\tilde{A}_z^q$ under the boundary condition that the electric field tangential to the waveguide surface is zero except at the slot region, where it is equal to the slot aperture electric field, i.e.

$$\begin{aligned} \tilde{A}_z^q &= \frac{jk_o}{\eta_o k_\rho^2} \tilde{E}_{q,z} \\ \frac{\partial \tilde{F}_z^q}{\partial n} &= \tilde{E}_{q,s} + \frac{jk_z}{k_\rho^2} \frac{\partial \tilde{E}_{q,z}}{\partial s} \end{aligned} \tag{15}$$

where 'n' is the unit normal vector directed away from the waveguide surface into the exterior region and 's' is the unit transverse vector along the waveguide surface in a counter-clockwise direction. For each spectral wave number k_z, eqn. 14 has to be solved subject to the boundary conditions given in eqn. 15. The resulting set of two-dimensional solutions is then inverse transformed to obtain the three-dimensional solutions in the spatial domain.

The finite difference method (FDM) is used for solving eqn. 14 in the exterior region. Since the domain of interest is an open region, the FD grid is truncated at some distance from the surface of the waveguide using the measured equation of invariance (Fig. 2). For each interior node, the standard central difference approximation of the differential operator is used. For the nodes corresponding to S_e, a five-point MEI is used [9, 13]. The external scattered magnetic field due to the qth expansion function of the magnetic current $\bar{f}_q^e$ is given by

$$\bar{\mathbf{H}}_q = \nabla \times A_z^q \hat{\mathbf{z}} - \frac{jk_o}{\eta_o} F_z^q \hat{\mathbf{z}} + \frac{1}{jk_o \eta_o} \nabla\nabla F_z^q \hat{\mathbf{z}} \tag{16}$$

The external admittance matrix elements are obtained by taking the inner product of the externally scattered magnetic field (eqn. 16) with respect to the weighting function $\tilde{\mathbf{f}}_p^e$. The (p, q)th element of the external admittance matrix is given by

$$Y_{pq}^{exp} = \int_{S_e} \bar{\mathbf{H}}_{ext}^{scat}(\bar{\mathbf{f}}_q^e)\bar{\mathbf{f}}_p^e da$$
$$= \frac{1}{2\pi}\int_{k_z}\int_{s_e} \tilde{\bar{\mathbf{f}}}_p^e(-k_z)\tilde{\bar{\mathbf{H}}}_{ext}^{scat}(\bar{\mathbf{f}}_q^e)dsdk_z$$
$$= \frac{1}{2\pi}\int_{k_z} \tilde{Y}_{pq}^{ext}(k_z)dk_z \qquad (17)$$

where 'da' denotes the differential area of the surface S_e and 'ds' denotes the differential length directed along the unit vector $\hat{\mathbf{s}}^e$.

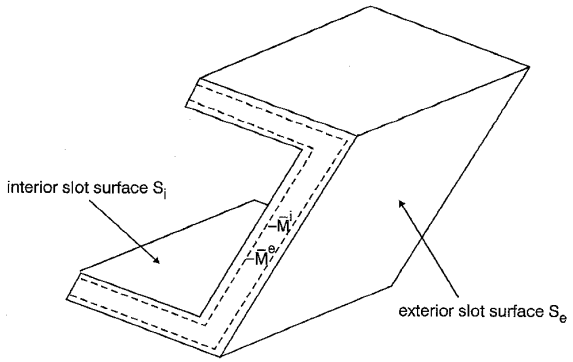

Fig. 3 *Cavity formed by the waveguide wall thickness used for computating cavity admittance matrix elements*

2.3 Computation of Y^c matrix elements

When the slot is cut on a waveguide with finite wall thickness, a cavity is formed with metallic walls on all sides (Fig. 3). The cavity is excited by equivalent magnetic currents placed on the surfaces S_e or S_i. As the shape of the cavity does not conform to standard geometries, a numerical approach has to be followed for computing the cavity fields. Here, the FD method is used for solving Helmholtz's equation for the electric vector potential, from which the cavity magnetic fields and the admittance matrix elements are computed. There is no need for absorbing the boundary as the domain of interest is a closed cavity. Helmholtz's equation for the electric vector potential $\bar{\mathbf{F}}$ is given by

$$\nabla^2\bar{\mathbf{F}}^q + k_o^2\bar{\mathbf{F}}^q = 0 \qquad (18)$$

where k_0 is the free-space wave number, subjected to the boundary condition $\hat{\mathbf{n}}^c \times \nabla \times \bar{\mathbf{F}}^q = \bar{\mathbf{f}}_q^{i,e}$ on the surface of the waveguide and $\hat{\mathbf{n}}^c$ is the unit surface normal vector pointing towards the interior of the cavity.

The cavity admittance matrix elements are given by

$$Y_{pq}^{mn} = \int_{S_m} \bar{\mathbf{f}}_p^m \bar{\mathbf{H}}(\bar{\mathbf{f}}_q^n)ds \qquad (19)$$

where

$$\bar{\mathbf{H}}(\bar{\mathbf{f}}_q^{i,e}) = \frac{1}{jk_o\eta_o}[k_o^2 + \nabla\nabla]\bar{\mathbf{F}}^q \qquad (20)$$

where $\bar{\mathbf{H}}(\bar{\mathbf{f}}_q^{i,e})$ is the magnetic field inside the cavity due to the qth basis function located at S_i or S_e as the case may be and $(m, n) = (i, e)$. $\bar{\mathbf{f}}_p^m$ corresponds to the pth weighting function on either the interior or the exterior surface as designated by 'm'. Similarly, $\bar{\mathbf{f}}_q^n$ corresponds to the qth basis function of the surface designated by 'n'.

3 Results

To validate the formulation presented in the previous Section, various test cases are examined in the X-band and in the S-band. In the numerical computations, the convergence of the solutions has been examined, and it is observed that around 15 basis functions are required to achieve satisfactory accuracy. The CPU time on a SUN sparc workstation for the computation of a single slot admittance is less than five minutes.

For the validation of the present theory, the resonant frequency and the resonant conductance are computed for three test cases and the results are tabulated (Table 1) for a WR90 waveguide with $w = 0.16$cm and $t = 0.124$cm. Also presented are the experimental and theoretical results of [6] and the corresponding percentage deviation from the experimental data. The frequency of operation is in the X-band and the slot tilts range from 20 – 30°. It is seen that as the slot tilt decreases, the percentage error of [6] is seen to be increasing and is of the order of 8% in the case of resonant conductance and is 1.7% in the case of resonant frequency. The error involved in the present method is of the order of 1% over the range of slot tilts. The computed resonant parameters are in close agreement with the experimental data.

The normalised conductance of the edge slot on a standard WR90 X-band waveguide at $f = 9.375$GHz is computed for varying slot tilts and fixed slot depth of cut $\delta = 0.35$cm in Fig. 4. Also presented are the experimental results [2] and the theoretical results of [6]. The results of both the theoretical approaches agree well with the experimental data for small slot tilts of the order of 10 – 15° when compared to larger slot tilts of 25 – 45°. For slot tilts less than 15°, the calculated conductance values are larger than the experimental data by around 1.5%. The deviation between the conductance of [6] and the measured data [2] is of the order of

Table 1: Resonant frequency and resonant conductance for three test cases

θ, deg.	δ, cm	Resonant frequency, GHz			Resonant conductance		
		experiment [6]	theory [6]	present theory	experiment [6]	theory [6]	present theory
20	0.304	10.08	9.91 (1.7%)	10.00 (0.9%)	0.0472	0.0512 (8.5%)	0.0477 (1.0%)
25	0.287	10.09	10.00 (0.9%)	10.03 (0.6%)	0.0801	0.0825 (3.0%)	0.0805 (0.5%)
30	0.260	10.07	10.01 (0.6%)	10.04 (0.3%)	0.1230	0.1271 (3.3%)	0.1240 (0.8%)

Data inside the brackets denote percentage variation from experimental values

6 – 8%. The results presented are for a fixed depth of cut δ = 0.35cm. For this case, the slot resonates for a tilt of 12°. For larger slot tilts of the order of 25 – 45°, the slot is operating away from resonance and there is around 35% deviation between the δ_{res} and δ = 0.35 cm. The present theory is still able to give better accuracy in this case and the conductance values are closer to the experimental data. The deviation between the conductance of [6] and the experiment [2] is more for larger slot tilts, which may be attributed to the use of 90° Green's functions for computing exterior fields. For larger slot tilts a significant portion of the slot lies on the narrow wall. As a result, the corners are strongly illuminated and also the area of slot sides increases leading to significant multiple reflections.

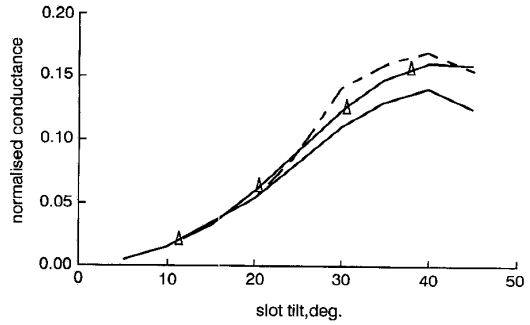

Fig. 4 *Normalised slot conductance against slot tilt for a fixed depth of cut δ = 0.35cm*
—Δ—Δ— present theory
——— experiment [2]
–·–·–·– reference [6]

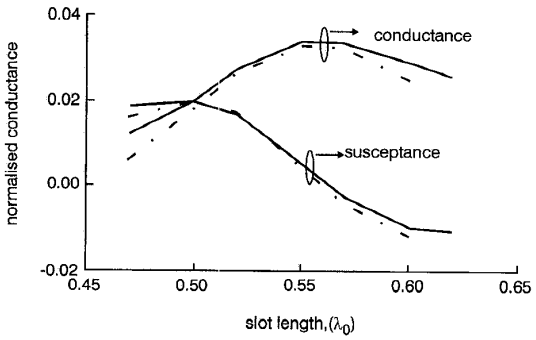

Fig. 5 *Normalised slot admittance against slot length for a fixed slot tilt θ = 15°*
——— present theory
–·–·–·– reference [6]

A test case is taken up in the X-band at f = 9.375GHz with a = 2.286cm, b = 1.016cm, w = 0.15875cm and t = 0.127cm. The slot tilt is maintained constant at θ = 15° and the shunt admittance of the slot is computed as a function of its length in Fig. 5. A set of curves obtained by Jan *et al.* [6] is also plotted for comparison. The present calculated results and that of [6] are relatively close for a slot length equal to the resonant length when compared to off-resonance points. The variation between the two theories is around 8% in resonant conductance and away from resonance it is as high as 20%. The present theory gives a relatively higher resonant length of 1.5% compared to that of [6]. Around the resonance point, the normalised admittance of both the theoretical approaches are close when compared to off-resonance points. The present theory gives higher values of conductance compared to [6]. It is seen that the effect of wall thickness is to increase the resonant length by more than 8%, which is significant in the design of edge slot arrays.

For a more elaborate validation of the present theory, the experimental determination of the admittance properties is taken up. Five test rigs are fabricated with the edge slot cut in a WR-284 waveguide having 0.1cm wall thickness. All the five test pieces have the same slot inclination of 15° and a slot width of 0.2cm, while the depth of cut δ in the broadwall is chosen as 0.238cm, 0.488cm, 0.738cm, 0.988cm and 1.238cm, respectively. The test rig with 0.238cm depth of cut is found to be defective and is rejected. The remaining four pieces satisfy the mechanical tolerances. The rigs are tested on HP8510B vector network analyser. To eliminate the effect of test flanges, the experiment is carried out in time domain with suitable gating of the signal around the position of the slot. The admittance of the slot is measured at 3.202GHz as a function of depth of cut and compared with the results of the present analysis (Fig. 6). It is seen that the theoretical results agree with the experimental results over a range of depth of cut. The resonant point is also predicted accurately. Extensive care is taken to minimise the experimental errors, but as the measured signal levels are low (around –30dB), typically a ± 0.5 – 1.0% error is expected in the measurements.

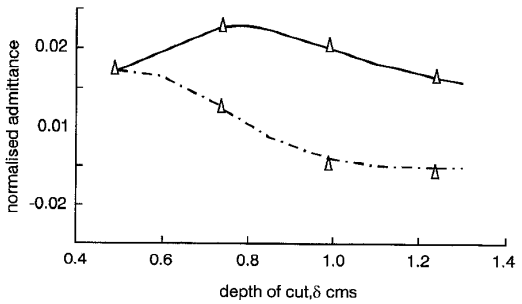

Fig. 6 *Slot admittance against depth of cut for a fixed slot tilt θ = 15° in the S-band*
——— conductance
–·–·–·– susceptance
Δ Δ Δ experiment

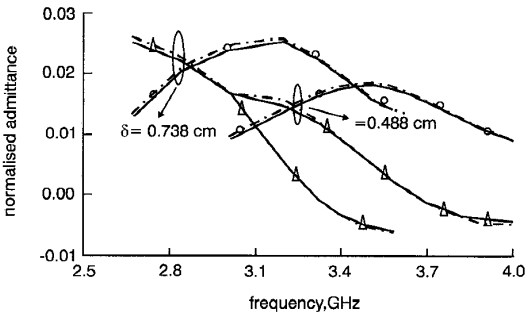

Fig. 7 *Normalised slot admittance against frequency for two different depths of cut*
——— theory
–·–·–·– experiment
O O O conductance
Δ Δ Δ susceptance

For the test case of δ = 0.488cm and δ = 0.738cm, the slot admittance is experimentally measured as a function of frequency and is presented in Fig. 7. The results of the present analysis are also plotted for comparison. As the depth of cut is increased from 0.488cm – 0.738cm, the resonant frequency goes down from 3.64GHz – 3.3GHz. This is expected as the slot length

increases with the depth of cut. It is found that the present analysis is able to give the resonant conductance within 1.5% of the experimental conductance. The percentage error in the resonant frequency is of the order of 0.5%. Close agreement between the theory and experiment is observed around the resonance point. Since the resonant frequency is affected significantly by the finite wall thickness and the coupling between the corners of the waveguide, the results are an indication of the validity of the present theoretical approach.

4 Conclusions

The admittance properties of the sidewall inclined slot in a rectangular waveguide are studied. A rigorous method of moments analysis with entire domain sinusoidal basis functions is applied for characterising the edge slot over a wide range of slot lengths. The finite wall thickness of the waveguide, the effects of the portion of the slot extending onto the broad faces, and the mutual interaction between the waveguide corners are incorporated into the formulation using S2DS and FD methods leading to an accurate solution of the edge slot problem. Results are presented for the admittance of the edge slot following the outlined theory and are found to be closer to the experimental results. The theoretical results are supported by previously published measured and theoretical data and also by the present experimental work.

5 References

1 STEVENSON, : 'Theory of slots in rectangular waveguides', *J. Appl. Phys.*, 1948, **19**, pp. 24–38

2 DAS, B.N., RAMAKRISHNA, J., and SARAP, B.K.: 'Resonant conductance of inclined slots in the narrow wall of a rectangular waveguide', *IEEE Trans.*, 1984, **AP–32**, pp. 759–761

3 HSU, P., and CHEN, S.H.: 'Admittance and resonant length of inclined slots in the narrow wall of a rectangular waveguide', *IEEE Trans.*, 1989, **AP–37**, pp. 45–49

4 JAN, C.G., HSU, P., and WU, R.B.: 'Moment method analysis of sidewall inclined slots in rectangular waveguide', *IEEE Trans.*, 1991, **AP–39**, pp. 68–73

5 JAN, C.G., and HSU, P.: 'Variational analysis of inclined slots in the narrow wall of a rectangular waveguide', *IEEE Trans.*, 1994, **AP–42**, pp. 1445–1458

6 JAN, C.G., WU, R.B., HSU, P., and CHANG, D.C.: 'Analysis of edge slots in rectangular waveguide with finite waveguide wall thickness', *IEEE Trans.*, 1996, **AP–44**, pp. 1120–1126

7 AHN, B.C.: 'Moment method analysis of narrow wall inclined slot on a rectangular waveguide'. PhD Thesis, University of Mississippi, MS, USA, 1992

8 WANG, H., and SANGSTER, A.J.: 'A hybrid analytical technique for radiating slots in waveguide', *J. Electromagn. Waves Appl.*, 1995, **9**, (5/6), pp. 735–755

9 PRAKASH, V.V.S., BALAKRISHNAN, N., and CHRISTOPHER, S.: 'Theoretical studies on the effect of waveguide geometry on the radiating slot'. 13th annual review of *Progress in applied computational electromagnetics*, ACES'97, Monterey, CA, USA, pp. 201–207

10 FOROORAGHI, , KILDAL, P.S., and RENGARAJAN, S.: 'Admittance of an isolated waveguide slot radiating between baffles using a spectrum of two-dimensional solutions', *IEEE Trans.*, 1993, **AP–41**, pp. 422–428

11 WETTERGREN, J., and KILDAL, P.S.: 'Admittance of a longitudinal waveguide slot radiating in to an arbitrary cylindrical structure', *IEEE Trans.*, 1995, **AP–43**, pp. 667–673

12 WETTERGREN, J., and SLATTMAN, P.: 'Electric field integral equation for cylindrical structures', *IEE Proc. Microw. Antennas Propag.*, 1996, **143**, pp. 147–151

13 MEI, K.K., POUS, R., CHEN, Z., LIU, Y.W., and PROUTY, M.D.: 'Measured equation of invariance: a new concept in field computations', *IEEE Trans.*, 1994, **AP–42**, pp. 320–328

14 PRAKASH, V.V.S., CHRISTOPHER, S., and BALAKRISHNAN, N.: 'On the application of Fourier transform techniques to waveguide interior regions', *J. Electro-Technol., SEE, India*, 1997, (accepted)